The Astrophysical Journal, 726:78 (8pp), 2011 January 10 doi:10.1088/0004-637X/726/2/78


# PHASE TRANSITION GENERATED COSMOLOGICAL MAGNETIC FIELD AT LARGE SCALES

Tina Kahniashvili[1,2,3], Alexander G. Tevzadze[3,4], and Bharat Ratra[5]
[1] McWilliams Center for Cosmology and Department of Physics, Carnegie Mellon University, 5000 Forbes Ave., Pittsburgh, PA 15213, USA; tinatin@phys.ksu.edu
[2] Department of Physics, Laurentian University, Ramsey Lake Road, Sudbury, ON P3E 2C, Canada
[3] Abastumani Astrophysical Observatory, Ilia State University, 2A Kazbegi Ave., Tbilisi 0160, Georgia; aleko@tevza.org
[4] Faculty of Exact and Natural Sciences, Tbilisi State University, 1 Chavchavadze Ave., Tbilisi 0128, Georgia
[5] Department of Physics, Kansas State University, 116 Cardwell Hall, Manhattan, KS 66506, USA; ratra@phys.ksu.edu
*Received 2010 May 30; accepted 2010 November 7; published 2010 December 16*

## ABSTRACT

We constrain a primordial magnetic field (PMF) generated during a phase transition (PT) using the big bang nucleosynthesis bound on the relativistic energy density. The amplitude of the PMF at large scales is determined by the shape of the PMF spectrum outside its maximal correlation length scale. Even if the amplitude of the PMF at 1 Mpc is small, PT-generated PMFs can leave observable signatures in the potentially detectable relic gravitational wave background if a large enough fraction (1%–10%) of the thermal energy is converted into the PMF.

*Key words:* cosmic background radiation – early universe – large-scale structure of universe – magnetic fields – turbulence

*Online-only material:* color figures

## 1. INTRODUCTION

A cosmological seed primordial magnetic field (PMF; generated during or prior to the radiation-dominated epoch) has been proposed to explain the existence of observed $\sim 10^{-6}$–$10^{-5}$ Gauss (G) magnetic fields (MFs) in galaxies and clusters (Widrow 2002; Vallee 2004). To preserve approximate spatial isotropy, a PMF has to be small and hence can be treated as a first-order term in perturbation theory. In the standard cosmological model (Ratra & Vogeley 2008), the energy density parameter of a PMF, $\Omega_B = \rho_B/\rho_{\rm cr}$, is significantly less than unity. Also, a PMF must be smaller than those observed in galaxies ($10^{-5}$ G), so $\Omega_B h_0^2 < 10^{-4}$ where $h_0$ is the Hubble constant in units of 100 km s$^{-1}$ Mpc$^{-1}$. Since the PMF energy density contributes to the radiation field, the big bang nucleosynthesis (BBN) bound implies $\Omega_B h_0^2 \leqslant 2.4 \times 10^{-6}$. The ratio of $\rho_B$ and the energy density of radiation $\rho_{\rm rad}$ is constant during cosmological evolution, if the PMF is not damped by a MHD (or other) process and so stays frozen into the plasma. Direct measurement of a cosmological MF is based on the Faraday rotation effect. A potential extension of this method, based on the rotation of the cosmic microwave background (CMB) polarization plane, appears promising (Kosowsky & Loeb 1996; Sethi 2003; Campanelli et al. 2004; Kosowsky et al. 2005; Giovannini & Kunze 2008; Kahniashvili et al. 2009). In addition, a PMF leaves imprints on the CMB temperature and polarization anisotropies (for a review see Giovannini 2006). Recently, two different groups (Neronov & Vovk 2010; Tavecchio et al. 2010) reported the detection of a lower bound on the large-scale correlated MF amplitude, of order $10^{-16}$–$10^{-15}$ G at 1 Mpc scale, through blazar observations.

In this paper, we consider cosmological PMFs generated by causal processes during phase transitions (PTs) such as the electroweak (EW) and QCD PTs (Harrison 1970; Vachaspati 1991; Brandenburg et al. 1996; Sigl et al. 1997; Joyce & Shaposhnikov 1997; Hindmarsh & Everett 1998; Grasso & Dolgov 2002; Boyanovsky & Simionato 2003; Campanelli & Giannotti 2005; Diaz-Gil et al. 2008; Stevens & Johnson 2009, and references therein). The main parameters of interest are the temperature $T_\star$ and the number of relativistic degrees of freedom $g_\star$ when the PMF is generated. We only use fundamental physical laws, such as conservation of energy, and how the MF interacts with the cosmological plasma through MHD turbulence, and do not make any assumption about the physical processes responsible for PMF generation. In contrast to earlier studies that estimate current limits on the PMF, we employ only energy conservation arguments without referring to specific processes responsible for transforming energy from a PMF to gravitational waves (GWs) or thermal or other forms of energy. We discuss cosmological signatures of such a PMF, including effects on the CMB temperature and polarization anisotropies and the production of GWs. We employ natural units with $\hbar = 1 = c$ and Gaussian units for electromagnetic quantities.

In Section 2, we define the spatial and temporal characteristics of the PMF and derive the BBN limits expressed in terms of the PT parameters. Results of our analysis are presented in Section 3, where we discuss the effects of a MF on the CMB temperature and polarization anisotropies and relic GWs. Conclusions are presented in Section 4.

## 2. MAGNETIC FIELD SPECTRUM

The maximal correlation length $l_{\rm max}$ for a causally generated PMF cannot exceed the Hubble radius at the time of generation, $H_\star^{-1}$. Hence $\gamma = l_{\rm max}/H_\star^{-1} \leqslant 1$, where $\gamma$ can be associated with the number of PMF bubbles within the Hubble radius, $N \propto \gamma^3$. The comoving length (measured today) corresponding to the Hubble radius at generation is inversely proportional to the temperature $T_\star$,

$$\lambda_{H_\star} = 5.8 \times 10^{-10}{\rm Mpc} \left(\frac{100\,{\rm GeV}}{T_\star}\right)\left(\frac{100}{g_\star}\right)^{1/6}, \qquad (1)$$

and is equal to 0.5 pc for the QCDPT (with $g_\star = 15$ and $T_\star = 0.15$ Gev) and $6 \times 10^{-4}$ pc for the EWPT (with $g_\star = 100$ and $T_\star = 100$ GeV), and the comoving PMF correlation length $\xi_{\rm max} \leqslant \lambda_H$. This inequality only accounts for the expansion of the universe while ignoring any possible effects of MHD turbulence (free turbulence decay or an inverse cascade if a helical PMF is present); this issue is addressed below.

If generated prior to BBN, the maximal value of the PMF energy density must satisfy the BBN bound, i.e., the total energy density of the PMF at nucleosynthesis $\rho_B(a_{\rm N})$ (where $a_{\rm N}$ is the scale factor at nucleosynthesis) should not exceed 10% of the radiation energy density $\rho_{\rm rad}(a_{\rm N})$. We first consider the simplest case when the PMF energy density evolves just due to the expansion of the universe. The conservation of the magnetic flux in this case leads to $\rho_B(t) \propto 1/a^4(t)$. Thus, the ratio $\rho_B/\rho_{\rm rad}$ is constant and the BBN constraint can be expressed as $\rho_B/\rho_{\rm rad}(a_\star) \leqslant 0.1$. Simple algebra gives that the maximal comoving value of the effective PMF $B^{(\rm eff)} = \sqrt{8\pi\rho_B} = 8.4 \times 10^{-7}(100/g_\star)^{1/6}$ G, if no PMF damping occurs before BBN. Even if the PMF energy is converted to another field contributing to the radiation (for example, GWs, Deriagin et al. 1987; Caprini & Durrer 2001), there is only $\rho_B(a_\star)$ magnetic energy available. The next issue is to determine how this energy is distributed at different wavelengths and the comoving PMF at a given comoving length scale $\lambda$. In this paper, we address this issue based on a phenomenological description of MHD processes in the early universe. Of course, for a scale-invariant (Ratra 1992; Bamba et al. 2008) or homogeneous PMF the limit remains the same at any scale. For any other PMF spectrum the limits are strongly scale dependent. As we will show below, the total PMF energy density is the physical quantity that has cosmological relevance. Obviously, from a limit on the PMF energy density we are able to reconstruct the effective value of the MF amplitude. Note that the maximal value of the PMF (from the BBN bound) is independent of the temperature at generation $T_*$, and depends only very weakly on the number of relativistic degrees of freedom at the moment of generation.

In this paper, we propose treating the initial PMF energy density $\rho_B$ as the magnetic energy density injected into the cosmological plasma at the comoving length scale $\lambda_0$. We justify our assumption that $\lambda_0$ should be identified as the size of the largest magnetic eddy by noting that the PMF is involved in MHD processes driven by turbulence. The typical length scale of the turbulence is determined by the PT bubble size. After generation, PMF evolution (during the PT) depends sensitively on the length scale under consideration. If the relevant timescales are shorter than $H_\star^{-1}$ we can neglect the expansion of the universe.[6] In this case, we must distinguish three sub-Hubble-radius regimes: $k_{H_\star} < k < k_0$ (where $k_{H_\star} = 2\pi/\lambda_{H_\star}$ and $k_0 = 2\pi/\lambda_0$; the large-scale decay regime); $k_0 < k < k_d$, with $k_d = 2\pi/\lambda_d$ the damping wavenumber scale related to plasma properties (the turbulence regime); and, $k > k_d$ (the viscous-damping regime). The interaction of the PMF with the plasma, and as a consequence the dynamics of the PMF, is sensitive to the presence of magnetic helicity (see Cornwall 1997; Giovannini & Shaposhnikov 1998; Field & Carroll 2000; Vachaspati 2001; Campanelli & Giannotti 2005; Diaz-Gil et al. 2008; Campanelli 2009 for magnetic helicity generation mechanisms). The expansion of the universe leads to additional effects. Most important among these are the additional damping of the PMF and the different time dependence of the growth rates for the comoving length scales ($L \propto a$) and the Hubble radius scale ($H^{-1} \propto t$, where $t$ is physical time). As a result, if a perturbation with wavenumbers $k$, $k_{H_0} < k < k_{H_\star}$, was outside the Hubble radius, at some time this perturbation will enter the Hubble radius (Tashiro et al. 2006).

The magnetic energy $E_M(k,t)$ and helicity $H_M(k,t)$ density power spectra are related to the magnetic energy and helicity densities through $\mathcal{E}_M(t) = \int_0^\infty dk E_M(k,t)$ and $\mathcal{H}_M(t) = \int_0^\infty dk H_M(k,t)$. The magnetic correlation length $\xi_M(t) = [\int_0^\infty dk k^{-1} E_M(k,t)]/\mathcal{E}_M(t)$ corresponds to the largest eddy length scale. All configurations of the MF must satisfy the "realizability condition" (Biskamp 2003; Verma 2004): $|\mathcal{H}_M(t)| \leqslant 2\xi_M(t)\mathcal{E}_M(t)$. Also, the velocity energy density spectrum $E_K(k,t)$ is related to the kinetic energy of turbulent motions through $\mathcal{E}_K(t) = \int_0^\infty dk E_K(k,t)$.

To account for the expansion of the universe we make use of the fact that conformal invariance allows for a description of MHD processes in the early universe by simply rescaling all physical quantities in terms of their comoving values and using the conformal time $\eta$ (Brandenburg et al. 1996; Banerjee & Jedamzik 2003, 2004). After this procedure, the MHD equations include the effects of the expansion while retaining their conventional flat spacetime form. To keep the description as simple as possible we work with dimensionless quantities, such as the already defined parameter $\gamma$ and the normalized wavenumber and normalized energy density defined below.

### 2.1. Magnetic Field Spatial Structure

We first consider the non-helical case. For a large enough Reynolds number the magnetic energy is redistributed by a Kolmogorov turbulence direct cascade. From the analogy between the Kolmogorov laws for hydrodynamic and magnetic turbulence, the magnetic energy dissipation comoving rate per unit enthalpy is $\varepsilon_M \simeq (2/3)^{3/2} k_0 v_A^3$, with $v_A = \sqrt{1.5\rho_B/\rho_{\rm rad}}$ being the effective Alfvén velocity corresponding to the total fluid-injected PMF energy, i.e., $\varepsilon_M = k_0(\rho_B/\rho_{\rm rad})^{3/2}$. In the absence of PMF damping at $k = k_0$, for Kolmogorov turbulence, $E_M(k) = C_M \rho_B k_0^{-1} \bar{k}^{-5/3}$ when $k_0 < k < k_d$, where $C_M$ is a constant of order unity ($C_M = 1.3 C_K$, where $C_K \simeq 1$ is the Kolmogorov constant), and $\bar{k} = k/k_0$ is the normalized wavenumber. At large scales when $k < k_0$ we model the PMF energy spectrum by a power law, $E_M(k) \propto k^\alpha$. Requiring continuity of the PMF spectrum at $k = k_0$, $E_M(k) = C_M \rho_B k_0^{-1} \bar{k}^\alpha$ for $k < k_0$. It is natural to assume that the MF energy injection scale $\lambda_0$ is the same as the maximal correlation length of the PMF, i.e., $\lambda_0 \simeq l_{\rm max} a_0/a_\star$.

The spectral index $\alpha$ of the largest scale MF energy density has been much discussed. Hogan (1983) requires causality of the field and argues that the PMF energy density spectrum must be white noise for scales larger than the causal horizon, $\lambda_0$. This corresponds to $\alpha = 2$. Durrer & Caprini (2003) claim that this violates the divergence-free PMF requirement and instead demand $\alpha = 4$. Both of these spectra, $\alpha = 2$ (Saffman) and $\alpha = 4$ (Batchelor),[7] are well known in the turbulence literature and, as discussed in Davidson (2004), their realization depends on initial conditions. In Kahniashvili et al. (2010a), the MF spectral shape at large scales was obtained from direct three-dimensional numerical simulations and $\alpha \in (2, 4)$ was found, depending on the initial conditions. Another possibility is Kazantsev's $\alpha = 3/2$ value, which can be rapidly achieved during the turbulence decay process discussed in Christensson et al. (2001) and Haugen et al. (2004). To keep the analysis as general as possible, we keep $\alpha$ arbitrary as much as possible.

[6] In the ideal case there is no magnetic energy damping due to the redistribution of the initial magnetic energy density $\rho_B(t_\star)$ through the different wavelength. To distinguish the initial magnetic energy present at a given scale from the total magnetic energy density right after redistribution, we define the magnetic energy density $\mathcal{E}_M$ and it is obvious that $\mathcal{E}_M \leqslant \rho_B$.

[7] $E \propto k^4$ is sometimes called the von Kármán spectrum.

Requiring $\mathcal{E}_M \leqslant \rho_B$, we obtain $C_M \leqslant 2(\alpha+1)/(3\alpha+5)$. With the nucleosynthesis requirement that the injected MF energy density must be smaller than 10% of the relativistic energy density, $\rho_B \leqslant 0.1\rho_{\rm rad}$,[8] and neglecting the contribution to the energy density from scales smaller than the viscous damping scale $\lambda_d$, for the maximal allowed value of $C_M$, we have $C_M\rho_B \leqslant 2.81\times10^{-14}C_{M,\max}(100/g_\star)^{1/3}$ G$^2$, and the magnetic energy spectrum

$$E_M(k) \leqslant \frac{5.2(\alpha+1)}{3\alpha+5}\left(\frac{100\ {\rm GeV}}{T_\star}\right)\left(\frac{100}{g_\star}\right)^{1/2} \times \gamma\frac{(10^{-9}{\rm G})^2}{{\rm pc}^{-1}}\begin{cases}\bar{k}^{\alpha} & \text{if}\quad \bar{k}<1\\ \bar{k}^{-5/3} & \text{if}\quad \bar{k}>1\end{cases}. \qquad (2)$$

Note that plasma properties determine the damping wavenumber $k_d$ that is defined by the Reynolds number Re $\gg 1$ of the fluid during the PT, $k_d = k_0{\rm Re}^{3/4}$. The plasma viscosity and other characteristics change during the evolution of the universe and also are scale dependent. That is, the Reynolds number is time and scale dependent, as shown in Figure 7 of Caprini et al. (2009b). Equation (2) accounts for the expansion of the universe. If the perturbation wavenumber is inside the inertial regime $k_0 < k < k_d$, it will always stay inside this regime, independent of the expansion.

Defining $B_\lambda$ as a smoothed PMF over a sphere of radius $\lambda$ ($\lambda > \lambda_0$) we have for the MF energy density on scales larger than the maximal correlation length, $\mathcal{E}_M^{\rm LS} = \int_0^{k_0} dk E_M(\bar{k}) = B_\lambda^2(k_0\lambda)^{\alpha+1}/[8\pi\Gamma(0.5\alpha+1.5)]$, where $\Gamma$ is the Euler Gamma function (Kahniashvili & Ratra 2007). This leads to the upper bound on $B_\lambda$,

$$\frac{B_\lambda}{10^{-9}{\rm G}}\left(\frac{\lambda}{1{\rm Mpc}}\right)^{(\alpha+1)/2} \leqslant \frac{2.28\times10^{-5\alpha-3}}{\sqrt{3\alpha+5}}\gamma^{(\alpha+1)/2} \times\left[8\pi\Gamma\left(\frac{\alpha+3}{2}\right)\right]^{1/2}\left(\frac{100\,{\rm GeV}}{T_\star}\right)^{(\alpha+1)/2}\left(\frac{100}{g_\star}\right)^{(\alpha+3)/12}, \qquad (3)$$

shown in Figure 1, for the EWPT with $T_\star = 100$ GeV and $g_\star = 100$ (upper panel) and the QCD PT with $T_\star = 150$ MeV and $g_\star = 15$ (lower panel). The parameter $\gamma$ is related to the PT duration parameter $\beta$ and the PT bubble wall speed $v_b$ as $\gamma = v_b\beta^{-1}H_\star$, and for a strong enough PT, with $v_b \to 1$, $\gamma \simeq \beta^{-1}H_\star$. Equation (3) is based on energy conservation and accounts only for the expansion of the universe. While previous studies (Hogan 1983; Banerjee & Jedamzik 2003, 2004; Caprini et al. 2009a, 2009b) address MF limits, the result shown here is independent of the MF generation model details, as well as those that govern the following magnetic energy transformation process dynamics. For the first time, we directly connect the MF strength limit to the characteristics of the PT: the bubble wall velocity $v_b$ and the duration of the PT. Both these enter through the parameter $\gamma$ which is dimensionless and independent of the expansion. Note that Equation (3) and, as a consequence, Figure 1 assume that $\rho_B(a_\star) \leqslant 0.1\rho_{\rm rad}(a_\star)$, thus any MF energy dissipation is neglected. In this sense, nucleosynthesis bound will be lower compared to the values shown in Figure 1, since any realistic calculation should include dissipation effects that

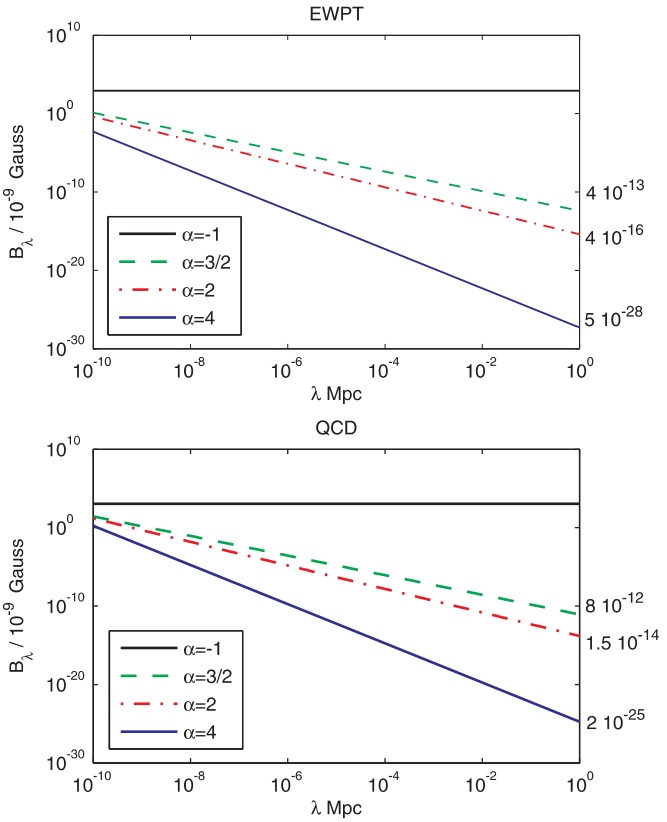


**Figure 1.** Maximal allowed $B_\lambda$ for a PMF generated during the EWPT (upper panel) with $T_\star = 100$ Gev, $g_\star = 100$, and $\gamma = 0.01$, and during the QCD PT (lower panel) with $T_\star = 0.15$ Gev, $g_\star = 15$, and $\gamma = 0.1$. Limits display the effect of the expanding universe. Realistic nucleosynthesis bounds need to include effects of MF damping.

(A color version of this figure is available in the online journal.)

can significantly reduce the MF amplitudes. On the other hand, Figure 1 is valid if the MF energy density is converted into a GW signal; also see Caprini et al. (2009a, 2009b).[9]

For the inflation-generated PMF ($\alpha \to -1$) the dependence on $T_\star$ and $g_\star$ disappear, and $B_\lambda \leqslant 10^{-6}$ G. As emphasized above the PMF limits shown in Figure 1 do not account for the non-cosmological evolution and damping of the PMF;[10] they address only the spatial structure of the PMF at large scales constrained by $\rho_B(t_\star) \leqslant 0.1\rho_{\rm rad}$. On the other hand, PMF damping would reduce the amplitude of the MF, so Figure 1 gives a real upper limit on the PMF. To avoid confusion we emphasize that these limits cannot be improved by the constraint from overproduction of GWs (Caprini & Durrer 2001), since only $\rho_B$ is available (at the moment of the PMF generation) to be transformed into another form of energy. The observable signatures of a PMF are also determined by the PMF total energy density and in this case the non-cosmological evolution of the PMF must be taken into account. Based on dimensional analysis we address the time evolution of the PMF in the next subsection, with

[8] We can extend the 10% bound to epochs earlier than nucleosyntheses. This is justified if the PMF was not damped away or MF energy was not transformed to another relativistic component, e.g., gravitational radiation (Caprini & Durrer 2001).

[9] Note that a limit qualitatively similar to that above can be obtained from considering the backreaction of the MF. A strong enough PMF will violate the isotropy of the Friedmann–Lemaître–Robertson–Walker metric. To be able to consider the PMF energy density as a first-order perturbation with respect to the radiation energy density at the moment of PMF generation, it is not unreasonable to assume that $\rho_B(t_\star) \leqslant 0.1\rho_{\rm rad}$. We thank the referee for emphasizing this point.

[10] Note that the simple dilution of the PMF due to the expansion of the universe is accounted for.

more precise numerical results presented in Kahniashvili et al. (2010a).

### 2.2. Magnetic Field Temporal Characteristics

The PMF spectrum is characterized not only by its spatial distribution, but also by its characteristic times: (1) the largest-size eddy turnover time $\tau_0 \simeq l_0/v_A$, which can also be used to determine the minimal duration of the source needed to justify use of the stationary turbulence approximation (Proudman 1952; Monin & Yaglom 1975); (2) the turbulence direct cascade timescale $\tau_{\rm dc}$; and (3) the large-scale turbulence decay time $\tau_{\rm ls}$.

We first consider the inertial range for which two timescales, $\tau_0$ and $\tau_{\rm dc}$, are relevant. For the EWPT ($\gamma \simeq 0.01$), and for reasonable moderate values of the Alfvén velocity ($v_A \leqslant 0.3$), the maximal size magnetic eddy turnover physical timescale $\tau_0 \simeq \gamma H_\star^{-1}/v_A$ is significantly shorter than the Hubble time $H_\star^{-1}$. As the universe expands, the eddy turnover time grows as $\tau_{\rm tr} \propto a$, since $v_A$ is a time-independent parameter and all length scales increase. The increased turnover timescale makes all MHD processes slower. We can effectively describe the expansion effects by considering MHD turbulence with a typical velocity that is decreasing as $\propto a^{-1}$. The time characteristic $\tau_{\rm dc}$ is determined by the proper dissipation rate $\bar{\varepsilon}_M$,[11] and it also increases as the universe expands. MHD turbulence decorrelation is a complex process (Terry & Smith 2007) that is currently not fully understood. To proceed we employ Kraichnan's approach (Kraichnan 1964) and specify decorrelation function $f_{\rm dc}[\kappa(k_{\rm ph}), \tau] = \exp\left[-\pi\kappa^2(k_{\rm ph})\tau^2/4\right]$ defined within the inertial range, $k_0 < k < k_d$. Here $\tau$ is the duration of the turbulence process, and $\kappa(k_{\rm ph}) = \bar{\varepsilon}_M^{1/3} k_{\rm ph}^{2/3}/\sqrt{2\pi}$ where $k_{\rm ph}$ is the physical wavenumber related to the comoving $k$ through $k_{\rm ph}(a) = ka_0/a$ ($a_0$ is the value of the scale factor now). Hence, we have

$$f_{\rm dc}[\bar{k}, \tau] = \exp\left[-\frac{2\pi^2}{9}\left(\frac{\tau}{\tau_0}\right)^2 \bar{k}^{4/3}\right]. \quad (4)$$

For non-helical turbulence, by considering the largest-size magnetic eddy decorrelation, $\tau_{\rm dc} \simeq 0.5\tau_0$, thus the direct cascade timescale is much shorter than the Hubble time, and this justifies the neglect of the expansion of the universe, as well as the assumption made above to neglect the energy density for $\lambda < \lambda_0$. Figure 2 shows the normalized PMF spectral energy density decays within one turnover time for perturbations within the inertial range. Note that the results presented in Figure 2 cannot be directly compared with those in Kahniashvili et al. (2010a), since Equation (4) assumes high enough Reynolds numbers while the numerical simulations are conducted at finite resolution leading to unrealistic, low Reynolds numbers.

Another characteristic time is related to the decay of large-scale turbulence. Large-scale turbulence processes are much slower than those occurring at smaller scales within the inertial range. Specific to this process is that there is no magnetic or hydrodynamic turbulence production source and free decay occurs. In this case, for consistency, we continue to use conformal time $\eta = \int dt/a$ and the normalized and comoving quantities. In the

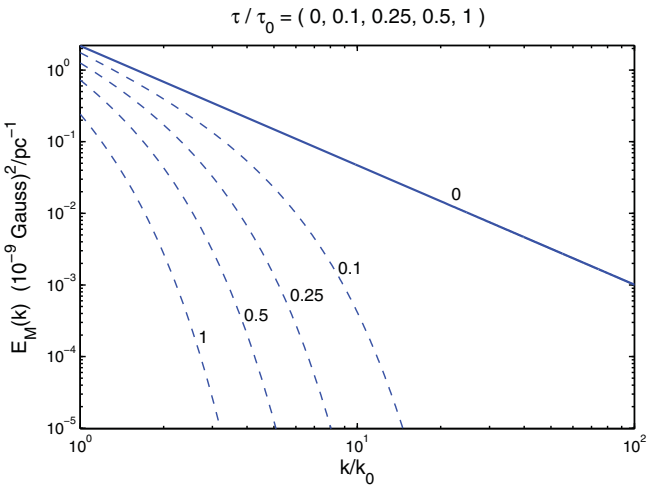


**Figure 2.** Spectral energy density $E_M(\bar{k})$ vs. normalized wavenumber $\bar{k}$ is shown during the freely decaying turbulence decorrelation process at different points in time: $\tau/\tau_0 = 0$, 0.1, 0.25, 0.5, and 1.0. Inertial range of the direct cascade turbulence spectrum is shown.

(A color version of this figure is available in the online journal.)

case of laboratory turbulence, to study large-scale decay one frequently assumes the grid turbulence decay law $k(t) \propto t^{-1.3}$ for perturbations with wavenumber $k(t) < k_G$, where $k_G = 2\pi/\lambda_G$ is the wavenumber corresponding to the grid scale $\lambda_G$ that can be associated with the correlation length (see, e.g., Pope 2000). In the expanding universe, the correlation length $\xi_M(\eta)$ and the Hubble radius length $\lambda_H(\eta) \simeq H^{-1}$ set natural length scales which are the analogue of the grid size in laboratory turbulence. On the other hand, the decay law in the expanding universe, according to Kahniashvili et al. (2010a), is substantially slower than in the laboratory case, i.e., $k(\eta) \propto \eta^{-1/2}$. A similar difference holds for the time evolution of the PMF energy density: the numerical simulations show $E_M(\bar{k}, \eta) \propto \eta^{-1}$ while the grid turbulence approach gives $E_M(\bar{k}, t) \propto t^{-n_G}$ with $n_G \in (1.13, 1.25)$ (Frisch 1975; Biskamp 1993).

Figure 3 shows the spatial and temporal surface of freely decaying turbulence at large scales ignoring MHD dynamo effects and neglecting all processes within the inertial range, $\bar{k} > 1$. Free decay is important only at large scales. As well as the grid turbulence analogy, the direct numerical simulations show that the PMF spectral energy density decreases much slower than the turbulence driven by the direct cascade. After free decay reduces the MF power substantially, the PMF on scales $k \ll k_0$ can be treated as a MF that is unaffected by turbulence. Of course, when considering realistic cosmological turbulence, in contrast to the laboratory turbulence case, the evolution of the fluid viscosity must be taken into account, which can change the PMF correlation length and energy density scaling laws shown here; see Caprini et al. (2009a) for a different model of free-decaying MHD turbulence. We also argue (Kahniashvili et al. 2010a) that free decay laws are very sensitive to the initial conditions, i.e., the free decay law depends on how the PMF was generated (Harrison 1970; Vachaspati 1991; Brandenburg et al. 1996; Sigl et al. 1997; Joyce & Shaposhnikov 1997; Hindmarsh & Everett 1998; Grasso & Dolgov 2002; Boyanovsky & Simionato 2003; Campanelli & Giannotti 2005; Diaz-Gil et al. 2008; Stevens & Johnson 2009, and references therein); whether the PMF was generated through bubble collisions, leading to $l_0 \simeq v_b\beta^{-1}$ with $v_b$ the bubble wall velocity and $\beta$ the bubble nucleation rate parameter ($\beta \simeq 100\, H_\star$

[11] Since, for the developed turbulence case, the magnetic energy proper dissipation rate per unit enthalpy must be approximately equal to the mean energy input rate per unit enthalpy of the source, i.e., the turbulence cascade timescale $\tau_{\rm dc} \simeq 2\pi\bar{\varepsilon}_M^{-1}(\rho_B/{\rm w}_{\rm rad}) \simeq \tau_0$, where $\rm w_{rad}$ is the radiation enthalpy (Kosowsky et al. 2002).

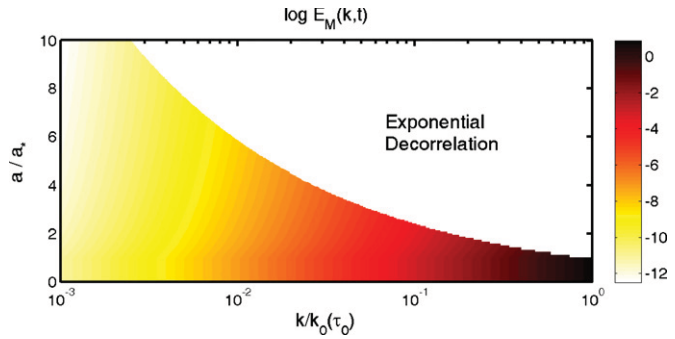


**Figure 3.** Spectral energy surface of the large-scale non-helical cascade turbulence $\log E_M(k, \eta)$. Free decay of turbulence starts at $\tau/\tau_0 = 1$.
(A color version of this figure is available in the online journal.)

for the EWPT) (Kahniashvili et al. 2010b), or if the PMF was present prior to the PT (Ratra 1992; Bamba et al. 2008). Another uncertainty comes from the kinetic (vortical) energy density spectrum $E_K$ (Christensson et al. 2001; Haugen et al. 2004).

The presence of even a small amount of magnetic helicity substantially affects PMF evolution (Biskamp & Muller 1999, 2000; Son 1999; Christensson et al. 2005; Banerjee & Jedamzik 2003, 2004; Campanelli 2007). If there is only a little magnetic helicity, first a direct cascade develops. At the end of this first stage the turbulence relaxes to a maximally helical state (Christensson et al. 2005; Banerjee & Jedamzik 2003) that satisfies $|\mathcal{H}_M(\eta)| \leqslant 2\xi_M(\eta)\mathcal{E}_M(\eta)$ and the second inverse cascade stage starts. Conservation of magnetic helicity implies that the magnetic energy density decays in inverse proportion to the correlation length growth during the inverse cascade. In contrast, for the case of well-established non-helical turbulence, the effect of magnetic helicity is still under discussion (Biskamp & Muller 1999, 2000; Son 1999; Christensson et al. 2005; Banerjee & Jedamzik 2003; Campanelli 2007). The main point of debate is related to the magnetic correlation length growth rate during the inverse cascade, i.e., $\xi_M(\eta) \propto \eta^{n_\xi}$, where the index $n_\xi$ is argued to be 1/2 (Biskamp & Muller 1999, 2000; Son 1999; Christensson et al. 2005) or 2/3 (Banerjee & Jedamzik 2003; Campanelli 2007). The total magnetic energy density $\mathcal{E}_M(\eta) \propto \eta^{-n_\xi}$, and the decay of large-scale kinetic energy $\mathcal{E}_K(\eta)$ (and as a consequence the ratio between the magnetic and kinetic energy densities $\mathcal{E}_M(t)/\mathcal{E}_K(\eta)$) are sensitive to $n_\xi$. In particular, Biskamp & Muller (1999, 2000), Son (1999), and Christensson et al. (2005) argue that $\mathcal{E}_K(\eta) \propto \eta^{-1}$, implying a faster decay of kinetic energy at large scales, while the results of Banerjee & Jedamzik (2003) and Campanelli (2007) lead to a constant $\mathcal{E}_M(\eta)/\mathcal{E}_K(\eta)$ within the inverse cascade and $\mathcal{E}_K(\eta) \propto \eta^{-2/3}$.

To compute the decay rate in physical time we use $t \propto \eta^2$. As in the case of non-helical turbulence, free decay here occurs over a longer period than when ignoring the expansion of the universe. Even so, in both these models, with $n_\xi = 1/2$ and $n_\xi = 2/3$, the kinetic turbulent energy density significantly decays on the EWPT timescale $H_\star^{-1}$, freezing the MF in the plasma, see Figure 4.

## 3. RESULTS AND DISCUSSION

The limits on the PMF at large scales are much stronger for the non-helical turbulence case; without the decay the constraint at zero redshift on 1 Mpc is $10^{-28}$ G for $\alpha = 4$ for an EWPT-generated PMF, see Figure 1 (also see Caprini et al. 2009a). In the $\alpha = 3/2$ case, the PMF can reach values of order $10^{-12}$ to $10^{-11}$ G that are required for seed MFs that might

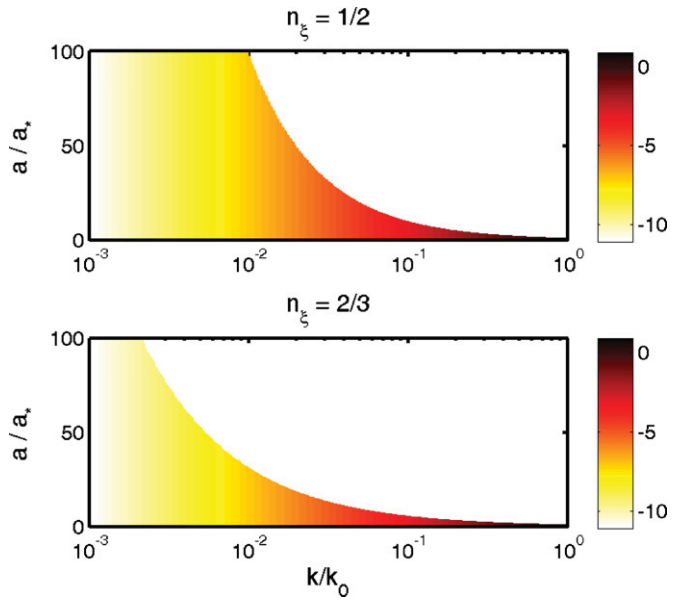


**Figure 4.** Spectral energy surfaces of the large-scale helical turbulence $\log E_M(k, \eta)$. The upper and lower panels correspond to the $n_\xi = 1/2$ and $n_\xi = 2/3$ decay laws.
(A color version of this figure is available in the online journal.)

be able to explain observed MFs in galaxies and clusters (Dolag et al. 2002). Again, the limits above correspond to the case when the PMF is frozen into plasma and no MHD processes are accounted for, of course, large-scale decay of turbulence will strengthen these limits for both the non-helical and helical cases. On the other hand, accounting for large-scale PMF decay the BBN bound does not imply $\rho_B \leqslant 0.1\rho_{\rm rad}$ when the PMF is generated. However, there is another requirement: the PMF cannot be the only component during the radiation-dominated epoch, thus $\rho_B/\rho_{\rm rad}(T_\star) < 1$. Even though our analysis is preliminary, it seems that a PT-generated PMF requires an effective amplification mechanism (such as a dynamo), or a specific initial condition, to act as a viable seed field for observed MFs in galaxies and clusters. Nonlinear processes during the PT can be responsible for the change of shape of the PMF at large scales and substantially long-duration turbulent sources can lead to significant magnetic power at large scales (Kahniashvili et al. 2010a).

A PT-generated PMF may have observable cosmological signatures. In what follows we examine two of them, CMB anisotropies and relic GWs. Before addressing the PMF cosmological signatures, let's consider the effective MF and the MF damping scale.

### 3.1. The Effective Magnetic Field and the Alfvén Damping Scale

As noted in Section 1, a stochastic MF can also be described by the effective MF value, $B^{(\rm eff)}$. Simple calculations allow us to connect both quantities, the smoothed MF $B_\lambda$ and $B^{(\rm eff)}$, through the following relation:

$$B^{(\rm eff)} = \frac{B_\lambda (k_D \lambda)^{(\alpha+1)/2}}{\sqrt{\Gamma(\alpha/2+3/2)}}, \quad (5)$$

where $k_D$ is the wavenumber cutoff above which the magnetic energy density spectrum $E_M(k)$ vanishes. In Section 2, we assumed that the PMF spectrum vanishes due to plasma viscosity

and so we considered a damping wavenumber $k_d$ determined by the Reynolds number.

On the other hand, there are different MHD processes that result in MF damping. In particular, Subramanian & Barrow (1998a, 1998b) and Jedamzik et al. (2000) study the damping of a homogeneous MF assuming the main dissipation process is Alfvén wave viscosity, resulting in $k_D^{-1} \simeq L_S v_A$, with $L_S$ being the Silk damping scale at recombination and $v_A$ determined by the background homogeneous PMF. For the case of a stochastic PMF (Mack et al. 2002),[12] define $k_D$ as

$$\left(\frac{k_D}{1\mathrm{Mpc}^{-1}}\right)^{\alpha+3} \approx 2\times 10^4 \left(\frac{B_\lambda}{10^{-9}\,\mathrm{G}}\right)^{-2} h \left(\frac{k_\lambda}{\mathrm{Mpc}^{-1}}\right)^{\alpha+1}, \quad (7)$$

so $k_D$ becomes $B_\lambda$, $\lambda$, and $\alpha$ dependent. Such a description must be used with caution. The picture of Alfvén wave induced dissipation requires that the effective background field be larger than the Alfvén wave associated field. On the other hand, when $\alpha \geqslant 0$, $B_\lambda$ with $\lambda > \lambda_D$ is significantly smaller than that associated with the fluctuating Alfvén wave MF, so we cannot treat the MF smoothed over the large-scale $\lambda$ as the effective background field even when the length scale $\lambda$ is comparable with the current Hubble radius. To avoid any possible confusion, it is useful to rewrite Equation (7) in a form independent of the $\lambda$ length scale and the smoothed value of the MF, $B_\lambda$. Using Equation (5), it is easy to see that

$$\frac{k_D}{1\mathrm{Mpc}^{-1}} = 1.4\sqrt{\frac{(2\pi)^{\alpha+1}h}{\Gamma\left(\frac{\alpha+3}{2}\right)}}\left(\frac{10^{-7}\mathrm{G}}{B^{(\mathrm{eff})}}\right). \quad (8)$$

In the case of the scale-invariant spectrum any dependence on the spectral index disappears (Equation (5)), and $B^{(\mathrm{eff})} = B_\lambda$. For the cutoff scale we have the following simple expression:

$$k_D = 1.4\ \mathrm{Mpc}^{-1} h^{1/2}\left(\frac{10^{-7}\mathrm{G}}{B^{(\mathrm{eff})}}\right). \quad (9)$$

The BBN limit ($B_{\mathrm{eff}} \leqslant 8.4\times 10^{-7}$ G) can be used to put an upper limit on the cut-off wavenumber scale in the case of the scale-invariant spectrum (i.e., with $n \to -3$), $k_D \geqslant 0.2$ Mpc$^{-1}$ ($\lambda_D \leqslant 36$ Mpc). For an extremely strong field that satisfies the BBN limit and with a white noise spectrum, $\alpha = 2$ (Hogan 1983), we have that $\lambda_D$ can be as large as 2.7 Mpc. Of course in this case it is inappropriate and unjustified to consider a PMF at 1 Mpc as is conventional, since at 1 Mpc there is no MF.

An important question is: how physical is a smoothed MF? At first glance it seems that it reflects the strength of the MF at a given scale. On the other hand, it is a tough task to compare $B_\lambda$ with observations. What the observations give is a measure of the MF in terms of effects it induces and the correlation length of MF. It is obvious that the smoothing scale and the correlation length are two different quantities. MF induced effects are not directly related to $B_\lambda$, rather they are strongly dependent on the MF spectral shape, correlation length, etc.

[12] Mack et al. (2002) defines the effective MF as the PM $\bar{B}_0$ smoothed over the damping length scale $L_D = 2\pi/k_D$, so

$$\bar{B}_0 = B_\lambda\left(\frac{k_\lambda}{k_D}\right)^{\frac{\alpha+1}{2}} \quad (6)$$

while in the present paper $B^{(\mathrm{eff})}$ is determined through the total energy of the MF. The difference is of order of few due to the prefactor $\sqrt{\Gamma(\alpha/2+3/2)}$ with $\alpha \in (-3, 2)$; see below.

Figure 1 shows the smoothed MF limits. One attempt to rule out a PMF with spectral shape $\alpha = 4$ was based on the extremely strong constraints on $B_\lambda$ at $\lambda = 1$ Mpc (Caprini & Durrer 2001). In some sense $B_\lambda$ reflects the normalization of the PMF and it is strongly model dependent (it depends on the choice of $n_B$ and $\lambda$), while the effective MF value $B^{(\mathrm{eff})}$ is a physical quantity that determines not only the total energy of MF but also the cosmological signatures of a PMF.

### 3.2. CMB Temperature and Polarization Anisotropies

A PMF induces CMB anisotropies. Usually, when considering PMF limits imposed by CMB data, one refers to the amplitude of the smoothed PMF $B_\lambda$ on large scales, typically $\lambda = 1$ Mpc (Giovannini 2006). On the other hand, when computing PMF induced CMB temperature and polarization anisotropy power spectra one finds $C_l \propto (B_\lambda^2\lambda^{\alpha+1})^2$ (Kahniashvili & Ratra 2007; Subramanian & Barrow 1998a, 1998b; Mack et al. 2002), and when considering Faraday rotation of the CMB polarization plane the rotation angle and the resulting B-polarization power spectra are $\propto B_\lambda^2\lambda^{\alpha+1}$ (Kosowsky et al. 2005; Kahniashvili et al. 2009). From the definition of $B_\lambda$ above, it is clear that PMF imprints on CMB fluctuations are determined by $\Omega_B$ (i.e., $[B^{(\mathrm{eff})}]^2$) or $\Omega_B^2$ (i.e., $[B^{(\mathrm{eff})}]^4$) (also see Jedamzik et al. 2000; Seshadri & Subramanian 2009).

On the other hand, the MF energy density varies due to the cosmological expansion, resulting in the time dependence of the damping wavenumber $k_D$. During a PT that generates the MF or when the MF starts to interact with the plasma (if it is generated prior to the PT), the total MF energy density at large scales is determined by the wavenumber of the peak of the MF spectral energy density, $k_0$. The value of this peak is fixed by the maximal correlation length of the MF at the PT, $\xi_M(\eta_s tar) = 2\pi/k_0$. In the simplest case that accounts only for the expansion of the universe and neglects all possible effects of magnetic helicity (the inverse cascade) or/and free turbulence decay, $\xi_M$ is independent of the evolution of the universe. In this case, during a PT all wavenumber $k < k_0$ modes contribute to the total MF energy density. The real time evolution is different: (1) in the absence of magnetic helicity the correlation length increases (i.e., the corresponding peak wavenumber $k_{\mathrm{peak}}(\eta) = 2\pi/\xi_M(\eta)$ shifts toward smaller values) due to large-scale turbulence decay $\xi_M(\eta) \propto \eta^{1/2}$, see Section 2.2; (2) the presence of magnetic helicity might make the correlation length grow faster, resulting in $\xi_M(\eta) \propto \eta^{2/3}$, see Section 2.2. While the correlation length increases, the energy density of the MF decreases. Additional damping is caused by Alfvén wave dissipation. The combined effect is that near the last-scattering surface some MF modes have been damped and dissipated and so the total MF energy density accounts for all modes with wavenumbers $k < k_D$.

The Alfvén wave damping scale $k_D \ll k_0$ and thus only a small part of the initial MF energy contributes to the CMB anisotropies. In particular, the CMB anisotropies are determined by $\rho_{\mathrm{CMB}} = (B^{\mathrm{eff}})^2/(8\pi) \propto B_\lambda^2(k_D\lambda)^{\alpha+1}$. The CMB anisotropies of the scale-invariant PMF (with $\alpha \simeq -1$) are determined only by the amplitude of the PMF and are independent of $\lambda$ and $k_D$. A scale-invariant PMF with amplitude larger than $10^{-9}$ G might leave observable CMB anisotropy traces (Yamazaki et al. 2008a, 2008b, 2008c, 2010). The situation is significantly different for a PMF with $\alpha > -1$. In this case, the main contribution to the MF energy density comes from small scales, and naively it might be expected that a PMF field with a smoothed amplitude at 1 Mpc lower than $10^{-9}$ G may not leave observable traces. In

reality the situation is more complicated. Even when the amplitude of the PMF is small enough, the contribution to the CMB anisotropies is not linearly dependent on $B_\lambda$. In particular, a PMF with $\alpha = 4$ and amplitude of order $10^{-13}$ G at 1 Mpc is constrained by CMB fluctuations (Mack et al. 2002). If we constrain the PMF by the CMB polarization plane rotation angle (Komatsu et al. 2010), then the limits on $B^{(\rm eff)}$ range over $10^{-8}$–$10^{-7}$ G for a PMF with spectral index $n_B \in (-3, 2)$ (Kahniashvili et al. 2010c). Of course, the smoothed amplitude $B_\lambda$ at 1 Mpc is very different if we compare an observationally allowed scale-invariant spectrum with an observationally allowed $n_B = 2$ spectrum. This has a very simple explanation: to get $B^{\rm eff} \sim 10^{-9}$ G for $\alpha > -1$, a lower value of $B_\lambda$ is required for $\lambda > \lambda_D$.

### 3.3. Relic Gravitational Waves

Another potentially interesting consequence of a PMF is relic GW generation (Deriagin et al. 1987; Caprini & Durrer 2001; Kahniashvili et al. 2008). The amplitude of these GWs is determined by the amount of MF energy density present at the PT and it is not affected by further MF damping. There have been a number of studies of turbulence-generated GWs and their detection prospects (see Kosowsky et al. 2002; Gogoberidze et al. 2007; Kahniashvili et al. 2008, 2010b; Caprini et al. 2009a, 2009b). The spectrum of GWs is very sensitive to the temporal and spatial characteristics of the source. Based on Figures 3 and 4 we argue here that the generation process is more effective within the PT timescale. This is because the amplitude of the source drops significantly outside the inertial range. The temporal decorrelation of the turbulence results in faster decorrelation of smaller eddies. Hence, the main contribution to the GW signal comes from the largest turbulent eddies, which can be associated with the length scale $\lambda_0$. To justify this conclusion we re-derive here the amplitude of direct-cascade MHD-turbulence-generated GWs. We do not consider the magnetic and kinetic turbulence sources separately, as previous work did (Kahniashvili et al. 2008), but instead consider them together and make use of the direct analogy between hydrodynamic and magnetic turbulence when equipartition is reached, i.e., $v_0 \simeq v_A$, where $v_0$ is the rms of the turbulence motion velocity. Note that to establish equipartition a few turnover times are required (Kahniashvili et al. 2010a). Hence, the stationary turbulence approximation is increasingly valid as compared to previous assumptions (Kosowsky et al. 2002). In contrast to earlier analysis (Gogoberidze et al. 2007; Kahniashvili et al. 2010b), we derive[13] the GW amplitude using dimensionless quantities independent of the expansion of the universe, and directly relate it to the PT $\gamma$ parameter,

$$h_C(f) \simeq 1.2 \times 10^{-15} v_A \gamma^{5/2} \left(\frac{100\,\mathrm{GeV}}{T_*}\right)\left(\frac{100}{g_*}\right)^{1/3} \times \left(\frac{f}{f_H}\right)^{1/2} S^{1/2}(f), \tag{10}$$

where $f$ is the frequency now and $f_H = \lambda_H^{-1} \simeq 1.6 \times 10^{-5}\,\mathrm{Hz}\,(g_*/100)^{1/6}(T_*/100\,\mathrm{GeV})$ is the Hubble frequency now.

[13] We make use of the aeroacoustic approximation analogy described in detail in Gogoberidze et al. (2007). The main assumption of our derivation is the long enough duration of turbulence. To make the result more physical we express all quantities in terms of the phase transition parameters.

Here $S(f)$ is determined by MF statistical properties,

$$S(f) = C_M^2 \int_1^{\mathrm{Re}^{3/4}} \frac{dx}{x^6} \exp\left(-\frac{f^2\gamma^2}{f_H^2 v_A^2 x^{4/3}}\right) \mathrm{erfc}\left(-\frac{f\gamma}{f_H v_A x^{2/3}}\right), \tag{11}$$

where $\mathrm{erfc}(x)$ is the complementary error function defined as $\mathrm{erfc}(x) = 1 - \mathrm{erf}(x)$, where $\mathrm{erf}(x) = \int_0^x dy \exp(-y^2)$ is the error function. As expected, the integral in Equation (11) is dominated by the large scale ($x \simeq 1$) contribution. Equations (10) and (11), presented here for the first time in such a simply interpretable form, allow us to straightforwardly estimate the strength of the GW signal if the energy density of the PMF is known. Also, Equation (11) clearly shows that the GW signal amplitude sensitively depends on $v_A$ which is one of the main parameters when considering GW detection prospects. This analytical estimate is in excellent agreement with the numerical estimates of Gogoberidze et al. (2007).

The amplitude and the energy density of the GW are related through

$$h_C(f) = 1.26 \times 10^{-18} \left(\frac{\mathrm{Hz}}{f}\right) \left[h_0^2\,\Omega_{\rm GW}(f)\right]^{1/2}, \tag{12}$$

where $\Omega_{\rm GW}(f)$ is the GW spectral energy density parameter. Using Equations (10) and (12), we have

$$\Omega_{\rm GW}(f) h_0^2 = 2.3 \times 10^{-4} v_A^2 \gamma^5 \left(\frac{100}{g_\star}\right)^{1/3} \left(\frac{f}{f_H}\right)^3 S(f). \tag{13}$$

Integrating $\Omega_{\rm GW}(f)$ over frequency, it can be seen that the efficiency of GW production is low, $\propto v_A^3\gamma^2$, with peak GW frequency for the EWPT being $f_{\rm peak} \simeq \gamma^{-1} v_A \lambda_H^{-1}$ (Gogoberidze et al. 2007) and an additional peak at $\lambda_H^{-1}$ for helical MHD turbulence (Kahniashvili et al. 2008), but the signal is potentially observable by LISA (Kahniashvili et al. 2008). For low frequencies $f \ll f_H$, $\Omega_{\rm GW} \propto f^3$ (also see Caprini et al. 2009a,b), and for high frequencies $f \gg f_H$ there is exponential damping. The peak amplitude $\Omega_{\rm GW}(f_{\rm peak}) = 2.3 \times 10^{-4} v_A^5 \gamma^2 (g_\star/100)^{-1/3}$ and is independent of $T_\star$. The analysis above shows that the main contribution to the GW background comes from the EWPT and we can ignore the expansion of the universe when studying GW generation (even for a helical PMF).

## 4. CONCLUSION

We have constrained a causally generated PMF produced prior to BBN, by using the BBN bound on the relativistic energy density during nucleosynthesis. The above analysis is independent of what kind of perturbations might be induced by the PMF, and whether the PMF acts as a long or short duration source for those perturbations (in particular, no overproduction of GWs occurs, which could lead to a strong constraint on the PMF amplitude, Caprini & Durrer 2001, 2005). We can also constrain a PMF generated after nucleosynthesis, but still during the radiation-dominated epoch, by requiring that the PMF energy density not be the dominant component. Figure 1 shows the PMF limits without accounting for damping or decay of the PMF. This is because PMF large-scale decay is very model dependent and comprehensive analysis requires correctly accounting for the initial conditions.

We have also argued that the direct use of a smoothed PMF $B_\lambda$ may cause confusion. We instead propose using the

PMF energy density when deriving constraints from PMF cosmological signatures. In particular, using $\xi_m(t) \propto t^{n_\xi}$ (where the correlation length is associated with the largest size MF eddy length $\lambda_0 = 2\pi/k_0$) together with $\mathcal{E}_M \propto t^{-n_E}$, in the framework of $\mathcal{E}_M^{\rm LS} \propto B_\lambda^2(\lambda k_0)^{\alpha+1}$, implies that $B_\lambda(t) \propto t^{((\alpha+1)n_\xi - n_E)/2}$, leading to $B_\lambda$ increasing if the smoothing scale $\lambda$ is fixed, while the real MF energy density is decreasing. It is obvious that $B_\lambda$ increasing in time is not a physical effect. Another advantage of using the PMF energy density is that the BBN limit does not depend on the energy scale at generation ($T_\star$), even though all characteristic length scales are strongly $T_\star$ dependent.

Free turbulence decays on large scales so, even without knowing the exact scaling law, this allows us to conclude that after the PT ends turbulence has been largely damped and so cannot produce gravitational radiation at the same level as that from the PT itself. At length scales larger than $\lambda_0$, even when the PMF energy is decaying slower than on small scales, the magnitude of the source is much lower due to the spectral energy density scaling ($\propto k^\alpha$) and no significant increase of GW generation efficiency can occur (even for a long-duration source; Caprini et al. 2009a). Accounting for this, the direct detection of relic GWs will allow us to study the PT MHD turbulence picture, if a sufficient fraction (1%–10%) of the thermal energy during the PT is present in the form of MF energy density.

We thank the anonymous referee for very useful comments. We appreciate helpful comments from A. Brandenburg and K. Jedamzik and useful discussions with C. Caprini, R. Durrer, S. Huber, L. Kisslinger, A. Kosowsky, T. Stevens, K. Subramanian, and T. Vachaspati. We acknowledge partial support from GNSF grant ST08/4-422, and DOE grant DE-FG03-99EP41043 and NASA grant NNXlOAC85G. T.K. acknowledges the ICTP associate membership program, and NORDITA for hospitality during the Electroweak Phase Transitions workshop.

## REFERENCES

Bamba, K., Ohta, N., & Tsujikawa, S. 2008, Phys. Rev. D, 78, 043524
Banerjee, R., & Jedamzik, K. 2003, Phys. Rev. Lett., 91, 251301
Banerjee, R., & Jedamzik, K. 2004, Phys. Rev. D, 70, 123003
Biskamp, D. 1993, Nonlinear Magnetohydrodynamics (Cambridge: Cambridge Univ. Press)
Biskamp, D. 2003, Magnetohydrodynamic Turbulence (Cambridge: Cambridge Univ. Press)
Biskamp, D., & Müller, W.-C. 1999, Phys. Rev. Lett., 83, 2195
Biskamp, D., & Müller, W.-C. 2000, Phys. Plasma, 7, 4889
Boyanovsky, D., Simionato, M., & de Vega, H. J. 2003, Phys. Rev. D, 67, 023502
Brandenburg, A., Enqvist, K., & Olesen, P. 1996, Phys. Rev. D, 54, 1291
Campanelli, L. 2007, Phys. Rev. Lett., 98, 251302
Campanelli, L. 2009, Int. J. Modern Phys. D, 18, 1395
Campanelli, L., Dolgov, A. D., Giannotti, M., & Villante, F. L. 2004, ApJ, 616, 1
Campanelli, L., & Giannotti, M. 2005, Phys. Rev. D, 72, 123001
Caprini, C., & Durrer, R. 2001, Phys. Rev. D, 65, 023517
Caprini, C., & Durrer, R. 2005, Phys. Rev. D, 72, 088301
Caprini, C., Durrer, R., & Fenu, E. 2009a, J. Cosmol. Astropart. Phys., JCAP11(2009)001
Caprini, C., Durrer, R., & Servant, G. 2009b, J. Cosmol. Astropart. Phys., JCAP12(2009)024
Christensson, M., Hindmarsh, M., & Brandenburg, A. 2001, Phys. Rev. E, 70, 056405
Christensson, M., Hindmarsh, M., & Brandenburg, A. 2005, Astron. Nachr., 326, 393
Cornwall, J. 1997, Phys. Rev. D, 56, 6146
Davidson, P. A. 2004, Turbulence (Oxford: Oxford Univ. Press)
Deriagin, D. V., Grigor'ev, D. Iu., Rubakov, V. A., & Sazhin, M. V. 1987, MNRAS, 229, 357
Diaz-Gil, A., Garcia-Bellido, A., Garcia Perez, M., & Gonzalez-Arroyo, A. 2008, J. High Energy Phys., JHEP07(2008)043
Dolag, K., Bartelmann, M., & Lesch, H. 2002, A&A, 387, 383
Durrer, R., & Caprini, C. 2003, J. Cosmol. Astropart. Phys., JCAP11(2003)010
Field, G. B., & Carroll, S. M. 2000, Phys. Rev. D, 62, 103008
Frisch, U., Pouquet, A., Léorat, J., & Mazure, A. 1975, J. Fluid Mech., 68, 769
Giovannini, M. 2006, Class. Quant. Grav., 23, R1
Giovannini, M., & Kunze, K. E. 2008, Phys. Rev. D, 78, 023010
Giovannini, M., & Shaposhnikov, M. E. 1998, Phys. Rev. D, 57, 2186
Gogoberidze, G., Kahniashvili, T., & Kosowsky, A. 2007, Phys. Rev. D, 76, 083002
Grasso, D., & Dolgov, A. 2002, Nucl. Phys. Proc. Suppl., 110, 189
Harrison, E. R. 1970, MNRAS, 147, 279
Haugen, N. E., Brandenburg, A., & Dobler, W. 2004, Phys. Rev. E, 70, 016308
Hindmarsh, M., & Everett, A. 1998, Phys. Rev. D, 58, 103505
Hogan, C. J. 1983, Phys. Rev. Lett., 51, 1488
Jedamzik, K., Katalinic, V., & Olinto, A. V. 2000, Phys. Rev. Lett., 85, 700
Joyce, M., & Shaposhnikov, M. E. 1997, Phys. Rev. Lett., 79, 1193
Kahniashvili, T., Brandenburg, A., Tevzadze, A. G., & Ratra, B. 2010a, Phys. Rev. D, 81, 123002
Kahniashvili, T., Campanelli, L., Gogoberidze, G., Maravin, Y., & Ratra, B. 2008, Phys. Rev. D, 78, 123006
Kahniashvili, T., Gogoberidze, G., & Ratra, B. 2008, Phys. Rev. Lett., 100, 231301
Kahniashvili, T., Kisslinger, L., & Stevens, T. 2010b, Phys. Rev. D, 81, 023004
Kahniashvili, T., Maravin, Y., & Kosowsky, A. 2009, Phys. Rev. D, 80, 023009
Kahniashvili, T., & Ratra, B. 2007, Phys. Rev. D, 75, 023002
Kahniashvili, T., Tevzadze, A., Sheti, S. K., Pandey, K., & Ratra, B. 2010c, Phys. Rev. D, 82, 083005
Komatsu, E., et al. 2010, arXiv:1001.4538
Kosowsky, A., Kahniashvili, T., Lavrelashvili, G., & Ratra, B. 2005, Phys. Rev. D, 71, 043006
Kosowsky, A., & Loeb, A. 1996, ApJ, 469, 1
Kosowsky, A., Mack, A., & Kahniashvili, T. 2002, Phys. Rev. D, 66, 024030
Kraichnan, R. H. 1964, Phys. Fluids, 7, 1163
Mack, A., Kahniashvili, T., & Kosowsky, A. 2002, Phys. Rev. D, 65, 123004
Monin, A. S., & Yaglom, A. M. 1975, Statistical Fluid Mechanics (Cambridge: MIT Press)
Neronov, A., & Vovk, I. 2010, Science, 328, 73
Pope, B. P. 2000, Turbulent Flows (Cambridge: Cambridge Univ. Press)
Proudman, I. 1952, Proc. R. Soc. A, 214, 119
Ratra, B. 1992, ApJ, 391, L1
Ratra, B., & Vogeley, M. S. 2008, PASP, 120, 235
Seshadri, T. R., & Subramanian, K. 2009, Phys. Rev. Lett., 103, 081303
Sethi, S. 2003, MNRAS, 342, 962
Sigl, G., Olinto, A. V., & Jedamzik, K. 1997, Phys. Rev. D, 55, 4582
Son, D. T. 1999, Phys. Rev. D, 59, 063008
Stevens, T., & Johnson, M. B. 2009, Phys. Rev. D, 80, 083011
Subramanian, K., & Barrow, J. D. 1998a, Phys. Rev. Lett., 81, 3575
Subramanian, K., & Barrow, J. D. 1998b, Phys. Rev. D, 58, 083502
Tashiro, H., Sugiyama, N., & Banerjee, R. 2006, Phys. Rev. D, 73, 023002
Tavecchio, F., Ghisellini, G., Foschini, L., Bonnoli, G., Ghirlanda, G., & Coppi, P. 2010, arXiv:1004.1329
Terry, W. P., & Smith, K. W. 2007, ApJ, 665, 402
Vachaspati, T. 1991, Phys. Lett. B, 265, 258
Vachaspati, T. 2001, Phys. Rev. Lett., 87, 251302
Vallée, J. P. 2004, New Astron. Rev., 48, 763
Verma, M. K. 2004, Phys. Rep., 401, 229
Widrow, L. M. 2002, Rev. Mod. Phys., 74, 775
Yamazaki, D. G., Ichiki, K., Kajino, T., & Mathews, G. J. 2010, Phys. Rev. D, 81, 103519
Yamazaki, D. G., Ichiki, K., Toshitaka, K., & Mathews, G. J. 2008a, Mod. Phys. Lett., 23, 1695
Yamazaki, D. G., Ichiki, K., Toshitaka, K., & Mathews, G. J. 2008b, Phys. Rev. D, 78, 123001
Yamazaki, D. G., Ichiki, K., Toshitaka, K., & Mathews, G. J. 2008c, Phys. Rev. D, 77, 043005